Survey of energetic O+ ions near the dayside mid-latitude magnetopause with Cluster

M. Bouhram, B. Klecker, G. Paschmann, S. Haaland, H. Hasegawa, A. Blagau, H. Rème, J.-A. Sauvaud, L. M. Kistler, A. Balogh

▶ **To cite this version:**

M. Bouhram, B. Klecker, G. Paschmann, S. Haaland, H. Hasegawa, et al.. Survey of energetic O+ ions near the dayside mid-latitude magnetopause with Cluster. Annales Geophysicae, 2005, 23 (4), pp.1281-1294. hal-00329397

HAL Id: hal-00329397
https://hal.science/hal-00329397

Submitted on 18 Jun 2008

HAL is a multi-disciplinary open access archive for the deposit and dissemination of scientific research documents, whether they are published or not. The documents may come from teaching and research institutions in France or abroad, or from public or private research centers.

L'archive ouverte pluridisciplinaire **HAL**, est destinée au dépôt et à la diffusion de documents scientifiques de niveau recherche, publiés ou non, émanant des établissements d'enseignement et de recherche français ou étrangers, des laboratoires publics ou privés.

Annales Geophysicae, 23, 1281–1294, 2005
SRef-ID: 1432-0576/ag/2005-23-1281
© European Geosciences Union 2005

Annales Geophysicae

Survey of energetic O^+ ions near the dayside mid-latitude magnetopause with Cluster

M. Bouhram[1,*], B. Klecker[1], G. Paschmann[1], S. Haaland[1], H. Hasegawa[2], A. Blagau[1,3], H. Rème[4], J.-A. Sauvaud[4], L. M. Kistler[5], and A. Balogh[6]

[1]Max-Planck-Institut für extraterrestrische Physik, D-85741 Garching, Germany
[2]Thayer school of engineering, Dartmouth College, Hanover, NH03755, USA
[3]Space Science Institute, R-76911 Bucharest, Romania
[4]CESR-CNRS, BP-4346, F-31028 Toulouse Cedex 04, France
[5]Space Science Center, University of New Hampshire, Durham, NH03824, USA
[6]Imperial College, London SW7 2AZ, UK
[*]now at: CETP-CNRS, 4 Avenue de Neptune, F-94100 Saint-Maur, France

Received: 12 August 2004 – Revised: 31 January 2005 – Accepted: 8 February 2005 – Published: 3 June 2005

Abstract. Since December 2000, the Cluster satellites have been conducting detailed measurements of the magnetospheric boundaries and have confirmed the unambiguous presence of ions of terrestrial origin (e.g. O^+) in regions adjacent to the dayside, mid-latitude magnetopause. In the present paper, we focus on the statistical properties of the O^+ ion component at energies ranging from 30 eV up to 40 keV, using three years of ion data at solar maximum from the Cluster Ion Spectrometry (CIS) experiment aboard two Cluster spacecraft. The O^+ density decreases on average by a factor of 6, from 0.041 to 7×10^{-3} cm^{-3} when crossing the magnetopause from the magnetosphere to the magnetosheath, but depends on several parameters, such as the geomagnetic activity or the modified disturbed storm time index ($D_{st}{}^*$), and on their location. The O^+ density is significantly higher in the dusk-side than in the dawn side region, which is consistent with the view that they originate mainly from the plasma sheet. A remarkable finding is that inward of the magnetopause, O^+ is the dominant contributor to the mass density 30% of the time on the dusk-side in comparison to 3% in the dawnside and 4% near noon. On an event basis in the dusk flank of the magnetopause, we point out that O^+ ions, when dominating the mass composition, lower the threshold for generating the Kelvin-Helmholtz instability, which may allow plasma exchange between the magnetosheath and the plasma sheet. We also discuss the effect of a substantial O^+ ion component when present in a reconnection region.

Keywords. Magnetospheric physics (magnetopause, cusp, and boundary layers; Magnetosphere-ionosphere interactions) – Space plasma physics (Discontinuities)

Correspondence to: M. Bouhram
(mehdi.bouhram@cetp.ipsl.fr)

1 Introduction

Since their first observation at magnetospheric altitudes by Shelley et al. (1972), it has been demonstrated that ions of unmistakably terrestrial origin (e.g. O^+) are continuously expelled from Earth's ionosphere and act as a significant source of plasma in the magnetosphere (e.g. Yau and André, 1997; Hultqvist et al., 1999). Long-term average data of O^+ ions at mid-altitudes (6000–24 000 km) and at speeds above the gravitational escape show that the outflow is solar cycle and geomagnetic activity dependent, with a global mean rate of the order of 7.2×10^{25} ions s^{-1} (Yau et al., 1988).

Although it is well established that ionospheric particles, as well as solar wind plasma, contribute to outer magnetospheric regions, to determine their relative contribution, supply routes and how much eventually escape from the magnetosphere is much more difficult. However, as pointed out by Seki et al. (2001), we may identify four escape routes for O^+ ions after flying out primarily from the high-latitude ionosphere that end in two distinct sides of the magnetosphere: (i) escape of cold ($<$10 eV) plasmaspheric particles or (ii) energetic ($>$1 keV) plasma sheet ions through the dayside magnetopause (MP), and (iii) escape through antisunward flow in the nightside plasma sheet or (iv) escape of tailward terrestrial ion beams through the lobe/mantle (L/M) region.

Recent observations from the Geotail satellites at large distances in the tail up to 210 Earth radii (R_E) have provided significant clues about escape routes through the nightside magnetosphere (Seki et al., 1998, 2001, 2002). In contrast, quantitative observations near the dayside MP or magnetosheath (MSH) for routes (i) and (ii) are poor. The first reports of O^+ ion observations at plasma sheet energies ($>$1 keV) near the dayside MP came from energetic ion composition measurements by Peterson et al. (1982), providing evidence that plasma transfer between the Earth and

the Sun occurs in both directions. A few case studies by Fuselier et al. (1989) in the subsolar low-latitude boundary layer (LLBL) under northward interplanetary magnetic field (IMF) conditions indicated the presence of two distinct O^+ populations, one from the plasma sheet at keV energies, and a new field-aligned O^+ beam of 100 eV injected directly from the high-latitude ionosphere. Other observations suggest that such ions have an originally cold component, coming from route (i), which become visible in the vicinity of the magnetopause upon acceleration/reflection by enhanced electric fields (Lundin and Dubinin, 1985; Sauvaud et al., 2001).

Two major mechanisms are usually invoked for magnetospheric ion escape across the dayside MP. Ions may escape along reconnected magnetic field lines (Speiser et al., 1981; Scholer, 1983) or continuously leak out simply because outer magnetospheric energetic ion drift paths intersect the dusk-side MP (Sibeck et al., 1987). Statistical studies using ion data without mass discrimination from past missions and the AMPTE/charge composition explorer (AMPTE/CCE) at the equatorial magnetopause (Sibeck et al., 1987) or from the Prognoz-10 satellite at low and mid-latitudes (Kudela et al., 1994) pointed out that the leakage of high-energy magnetospheric ions (>5 keV) supplies most of the ions observed in the MSH at such energies. Using ion composition measurements by AMPTE/CCE in the MSH in the energy range of 0.1 to 17 keV, Fuselier et al. (1991) showed that the occurrence of the O^+ leakage is 10 to 20% of the time, with an average O^+ density of less than $10^{-2}\,cm^{-3}$. However, this study was restricted to the subsolar MSH and large solar wind pressure conditions, because of the low apogee ($8.8\,R_E$) of AMPTE/CCE. The arrival of a solar wind pressure pulse is known to account for a significant escape of O^+ ions, which form layered structures in the MSH following the magnetosphere compression (Zong and Wilken, 1998).

Because the flux in energetic magnetospheric ion pitch-angle distributions peaks strongly near 90°, one expects leakage to occur primarily at equatorial latitudes, and since the bulk of magnetospheric ions are trapped near the equator, only fewer ions would be able to escape at higher latitudes (Sibeck et al., 1987). However, a recent case study with the Cluster multi-satellite system reveals continuous escape of energetic (>10 keV) O^+ ions across the mid-latitude ($\sim$30°) dusk-side MP, at velocities which depend strongly on the orientation of the MSH magnetic field (Marcucci et al., 2004). These observations, along with modeling studies, suggest that ions simply escape because of their finite gyroradius (>1000 km), provided the MSH convection and magnetic field orientation are taken accordingly into consideration. In another case study by Phan et al. (2004) at the dusk-side, mid-latitude MP, reconnection jets were observed by Cluster in correlation with substantial densities (0.2–0.3 cm^{-3}) of high-energy (>3 keV) O^+ ions in every jet, that would indicate continuous reconnection for more than 2 h under steady southward IMF conditions.

Because composition measurements directly impact the transfer mechanisms across the MP, investigating the O^+ ion content at the MP is not only useful to estimate the atmospheric loss rate and to access sources of plasma, it also acts as a powerful tool to probe the physical processes which are involved (Eastman and Christon, 1995). In particular, many of the tests, such as the tangential stress balance or the criterion for Kelvin-Helmholtz (KH) instability, both applied to data obtained across the MP, involve the mass density of the plasma. Therefore, in the absence of mass-resolved measurements, assumptions about the ion composition have had to be made.

The purpose of the paper is to investigate statistically the characteristics of the O^+ distributions observed in the near-MP regions using three years of data aboard two Cluster spacecraft. After presenting two events associated with substantial fluxes of O^+ ions, we investigate the influence of the geomagnetic activity on this O^+ contribution, and discuss its potential role in affecting physical processes, such as the KH instability or magnetic reconnection.

2 Instrumentation and data analysis

2.1 Sources of data

The four identical Cluster satellites, SC1, SC2, SC3 and SC4, have an elliptical orbit ($4.0\times19.6\,R_E$) with an inclination of 90°. Particle data shown here are from the Cluster ion spectrometry (CIS) experiment (Rème et al., 2001), which comprises two analyzers. First, a hot ion analyzer (HIA) that measures three-dimensional ion distributions over the energy range 5–32 000 eV, without mass discrimination, by combining a classical, symmetric, quadrispherical analyzer with a fast particle imaging system, based on a microchannel plate, electron multipliers and position encoding discrete anodes, operates aboard two satellites, SC1 and SC3. Second, the composition and distribution function (CODIF) analyzer that measures 3-D distributions of the major ion species over the energy range 30–40000 eV, operates aboard three satellites, SC1, SC3 and SC4. It is a combination of a top-hat energy per charge (E/Q) analyzer followed by a post acceleration of 15 kV and a time of flight (TOF) measurement. The E/Q analyzer is divided into two halves, with a geometrical factor different by a factor of 100. Only one half operates at a time, selected by time-tagged commands, giving a 180° instantaneous field-of-view divided into 8 sectors of 22.5° each. The E/Q analyzer sweeps through the full energy range 32 times per spin, so that the full distribution is obtained in one spin (4 s). In practice, depending on the telemetry product, the time resolution of O^+ ion distributions ranges from 1 to 12 spins, i.e. from 4 to 48 s, respectively.

Note that under periods of strong ion fluxes, such as within the magnetosheath, the count rate can be rather high and needs to be corrected, depending on the time constants of the electronics (dead-time correction). Because the electronics of HIA is much faster than that of CODIF, and the dead-time correction is done on board for HIA and not for CODIF, it was preferable for the present study to utilize CODIF for O^+ measurements, and to infer H^+ moments from HIA on-board

moments after subtracting the O^+ contribution and assuming a fraction of He^{++} ions (see Appendix A for details). Note also that in the magnetosheath, O^+ measurements suffer from spurious counts at energies below 3–10 keV, due to the contamination from high H^+ fluxes, which have to be excluded in the moment computation. However, detailed inspections of the TOF histograms usually reveal that the O^+ population does not extend below 3 keV, so we decided to compute O^+ moments above 3 keV, which is usually much higher than the H^+ mean energy in the magnetosheath (typically 0.3 keV). However, one cannot exclude for all data sets the possibility that a cold O^+ component exists at low-energy but is not measurable by CODIF. Hence, we will focus for the rest of the paper on the high energy (>3 keV) O^+ component.

The magnetic field data utilized in the present study originate from the fluxgate magnetometer (FGM) installed aboard all Cluster spacecraft (Balogh et al., 2001). Finally, solar wind parameters from the Wind and Advanced Composition Explorer (ACE) missions and measurements of the K_p and D_{st} indexes are available from the OMNIWeb system of the National Space Science Data Center in hourly intervals for statistical studies. Here, solar wind parameters are time-lagged using the solar wind speed and the satellite locations in the solar wind to account for the delay for the plasma to reach the MP (see http://nssdc.gsfc.nasa.gov/omniweb/html/omni2_doc.html for details).

2.2 Selection of near-magnetopause regions

The Cluster fleet explores various plasma regions, such as the magnetosheath (MSH), magnetopause (MP), and adjacent magnetospheric regions, such as the lobe/mantle, the exterior cusp, the low-latitude boundary layer (LLBL), or the plasma sheet boundary layer (PSBL) on the flanks. This depends on the orbit, as shown schematically in Fig. 1, where we have drawn Cluster trajectories in an aberrated-displaced $x-y$ coordinate system for model boundaries (See Fig. 10.3 of Paschmann and Daly, 2000) for three individual events which are discussed in Sect. 3. In practice, automatic examination of the MP itself is difficult, partly due to its unsteadiness, and partly due to the limited temporal resolution of the particle data (>4 s) compared to the average time needed to cross the region (<30 s). Conversely, the study of the near-MP magnetosheath region does not suffer from temporal-resolution limitations, since the region under consideration is much wider (see Phan et al., 1995). The same is true for the adjacent magnetospheric regions. Therefore, we have defined for each pass four distinct regions; Eq. (1) the magnetosheath proper, Eq. (2) the magnetosheath boundary layers (MSHBL), Eq. (3) the magnetospheric boundary layers (MSPBL) (i.e. LLBL, PSBL or cusp entry layer), and (4) the magnetosphere (MSP).

The flowchart of Fig. 2 describes the automated routine based on CIS measurements and used to identify those regions. First, we select a time interval around the MP ($\pm 2\ R_E$) using the MP model from Shue et al. (1997), which depends

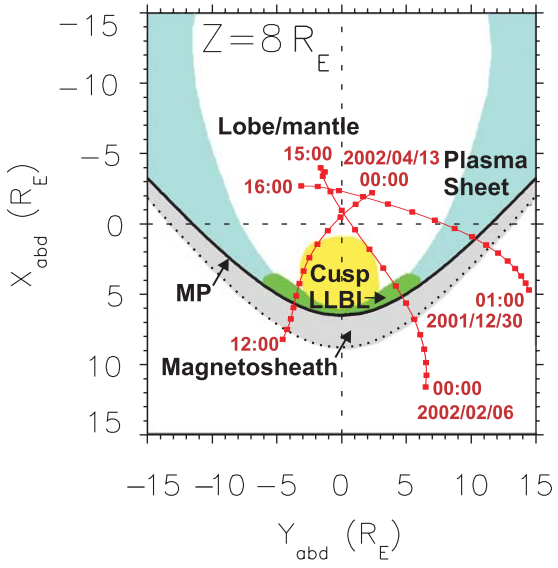

Fig. 1. Examples of trajectories (red curves with points separated by one-hour intervals) of Cluster in the aberrated-displaced $X-Y$ plane at $|z|$=8 R_E. The three examples correspond to the individual events which are discussed in Sect. 3. The magnetopause location is inferred from the model of Shue et al. (1997), using a mean solar wind pressure of 2 nPa and a southward component of the interplanetary magnetic field set to 0.

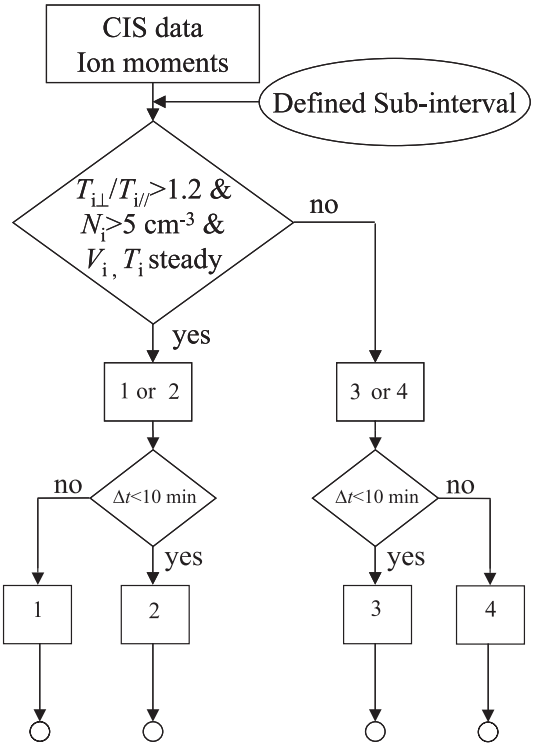

Fig. 2. Flowchart describing the procedure we have utilized to identify near-magnetopause time intervals: Eq. (1) magnetosheath proper, Eq. (2) magnetosheath transition layers, Eq. (3) magnetospheric transition layers, and (4) magnetosphere.

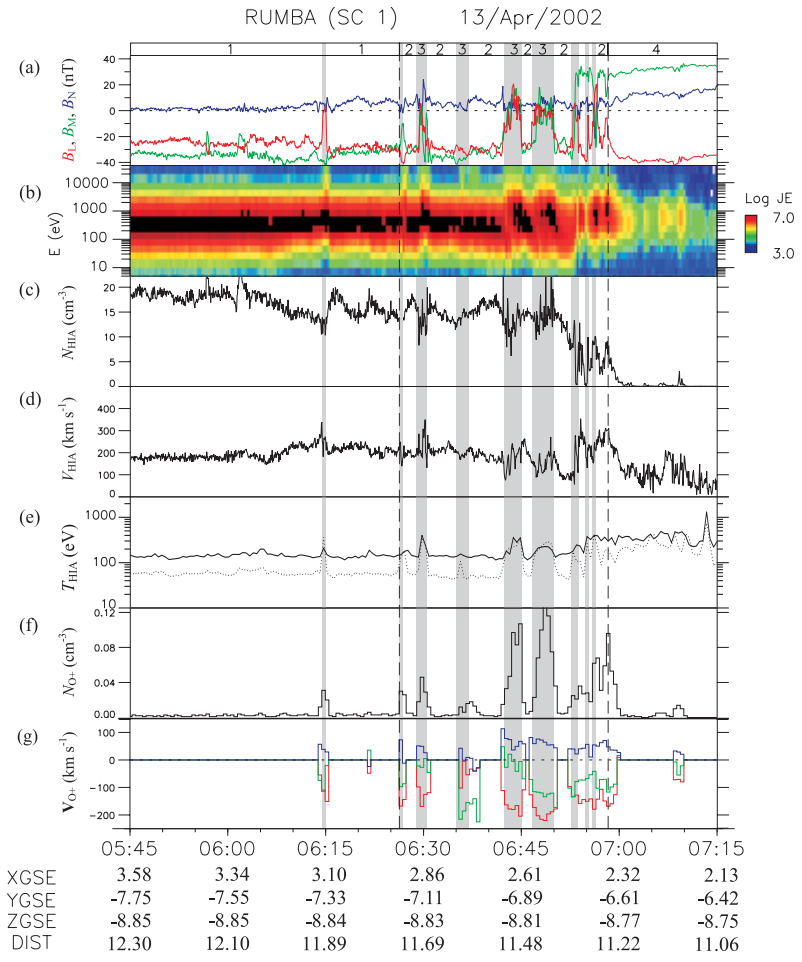

Fig. 3. Measurements in the magnetosheath/MP/magnetosphere from Cluster SC1 on 13 April 2002. (**a**) Magnetic field components in the LMN frame, (**b**) ion energy-time spectrogram in Log [eV/(s cm^{2}sr eV)] from HIA, (**c**) ion number density in cm^{-3} from HIA, (**d**) ion flow speed in km s^{-1} from HIA, (**e**) parallel (dot) and perpendicular (solid) ion temperatures from HIA, (**f**) O^+ number density in cm^{-3}, (**g**) O^+ velocity components in the LMN coordinate system in km s^{-1}. L, M, and N components are plotted in red, green and blue, respectively. A region identifier bar at the top sorts intervals of Eq. (1) magnetosheath proper, Eq. (2) magnetosheath transition layers, Eq. (3) magnetospheric transition layers (also in gray), and (4) magnetosphere.

on the hourly solar wind dynamic pressure P_{SW} and B_z component of the interplanetary magnetic field (IMF). Then, we focus on the magnetosheath intervals because they may be easily identified from the plasma moments using the criteria of Fig. 2, since the combination of the ion density and the temperature anisotropy has intrinsic characteristics, being higher there than anywhere else. To identify whether the spacecraft enters a layer adjacent to the MP (2 or 3) or the proper region itself (1 or 4), we do a test with respect to the dwell time of the crossing, which is set to 10 min. We choose this value because it corresponds roughly to the time Δt needed by the spacecraft to travel a distance $L_\perp$ of about 2 ion gyroradii, taking a perpendicular temperature of 2 keV and a B-field magnitude of 30 nT. Here, if the dwell time does not exceed 10 min, then the encounter is considered as a valid sample of a boundary layer. We should also note that because of the limited temporal resolution of the CIS instruments, only transition layer crossings longer than 15 s are considered. Finally, we have to check for consistency that for an inbound (outbound) crossing, the spacecraft travels from region 1 (region 4) to region 4 (region 1), while regions 2 and 3 should be observed in between. In Sect. 3, we show results of the region identification technique, when applied to specific events.

3 Individual events

3.1 13 April 2002 case

Figure 3 shows one Cluster-SC1 inbound pass through the mid-latitude dawn flank of the MP that occurred on 13 April 2002. Magnetic field components from FGM have a 4-s resolution and are in the boundary normal coordinate system LMN (Russell and Elphic, 1979). This system is defined such that the $\boldsymbol{N}$ vector points outward along the MP normal, and the ($\boldsymbol{L}$, $\boldsymbol{N}$) plane contains the GSM z axis. The

MP normal direction was determined using the model of Shue et al. (1997), using a mean solar wind dynamic pressure P_{SW}=1.9 nPa, as measured by ACE. The ion (without mass discrimination) and O^+ data are from HIA and CODIF with a resolution of 4 and 32 s, respectively. As the spacecraft moves slowly from the MSH to the MSP in the $Z_{GSE}\sim-8.8\ R_E$ plane, different regions may be identified. SC1 is originally in the MSH proper (region 1), as evidenced by the observation of a cold and dense (15–20 cm^{-3}) ion population in Figs. 3c and d with a significant temperature anisotropy, while magnetic field data indicate that the IMF is steadily southward with a strong duskward component. Around 06:15, 06:26 and 06:30 UT, SC1 enters the MSPBL briefly, as evidenced by sudden increases in the ion temperature and drops in the ion density, as well as changes in the magnetic field orientation. Some of these crossings are correlated with the presence of high-speed plasma jets near the MP, as evidenced in Fig. 3d by an increase in the HIA velocity relative to the velocity in the adjacent MSHBL. Such plasma jets when correlated with a change in the B-field orientation may be used as a signature of plasma acceleration due to magnetic stresses (see, for example, Paschmann, 1997), indicating that reconnection is occurring or has already occurred. Between 6:40 and 7:00 UT, SC1 encounters the MSPBL several times, as identified by the rotation of the B_L and B_M components of the magnetic field. After 7:00 UT, SC1 passes into the lobe/mantle (L/M) region as evidenced by less dense, magnetosheath-like, dispersive flows with a bulk velocity mainly parallel to $\boldsymbol{B}$ (not shown). The last two panels reveal the presence of substantial densities (up to 0.13 cm^{-3}) of O^+ ions, which correlates very well with partial magnetosphere excursions up to 7:00 UT, and represents up to 10% of the mass density. Because the O^+ velocity $\boldsymbol{V}_O$ exhibits a component opposite to the $\boldsymbol{L}$ direction in the Southern Hemisphere, it is obvious that such ions are traveling from the equatorial plasma sheet and drifting out of the dawnside MP because of a positive $\boldsymbol{N}$ velocity component.

Figure 4 provides a detailed examination of the O^+ distribution functions in the ($\boldsymbol{N}$, $\boldsymbol{L}$) plane at $<V_M>$ and in the ($\boldsymbol{N}$, $\boldsymbol{M}$) plane at $<V_L>$, as a function of energy at two different times. A sketch of ion orbits is given in Fig. 5 to explain the shape of the velocity distributions. At 6:44:43 UT, SC1 is in the MSPBL (region 3) and shell-like distributions centered along the B-field direction (close to $\pm\boldsymbol{L}$) but broadly extended perpendicularly to $\boldsymbol{B}$ are observed with velocities ranging from 200 up to 700 km s^{-1}. For B=50 nT, this corresponds to O^+ gyroradii between 600 and 2400 km and therefore larger than the typical MP thickness inferred from multispacecraft methods, which ranges from 200 to 1000 km (Haaland et al., 2004). At 6:46:20 UT, SC1 is in the MSHBL (region 2) and truncated O^+ distributions are observed, i.e. only in the half-plane $V_M<0$. This corresponds to O^+ ions with their gyrocenter G_1' or G_2' inside the MP or magnetosphere and reaching the magnetosheath at P' because of their large gyroradius. As shown in Fig. 5b, where we neglect the effect of the convection drift, because of the southward

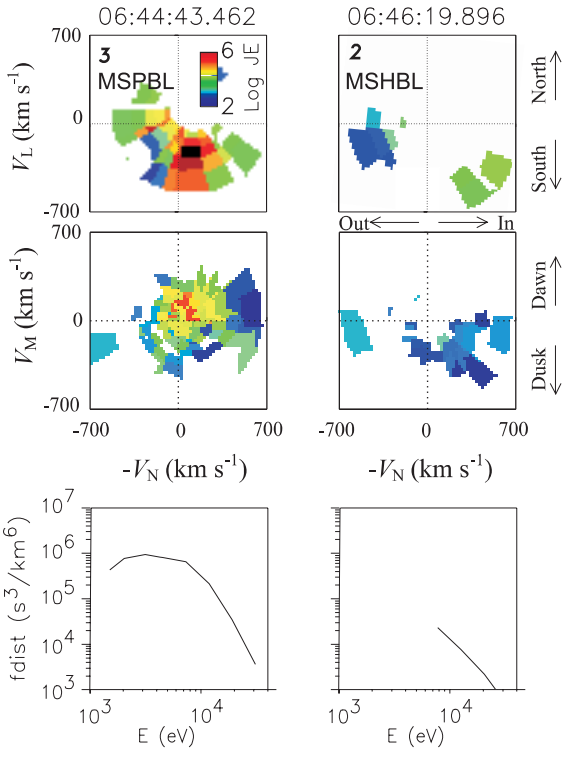

Fig. 4. From top to bottom, cutaway of the O^+ distribution function in the ($\boldsymbol{N}$, $\boldsymbol{L}$) plane at $V_M=<V_M>$ in Log[eV/(s cm^2 sr eV)], in the ($\boldsymbol{N}$, $\boldsymbol{M}$) plane at $V_L=<V_L>$ in Log[eV/(s cm^2 sr eV)], and solid-angle averaged distribution function in s^3 km^{-6} versus energy. The number in the topleft-hand side corner of each velocity distribution plot in the ($\boldsymbol{N}$, $\boldsymbol{L}$) plane refers to the region, according to Fig. 3.

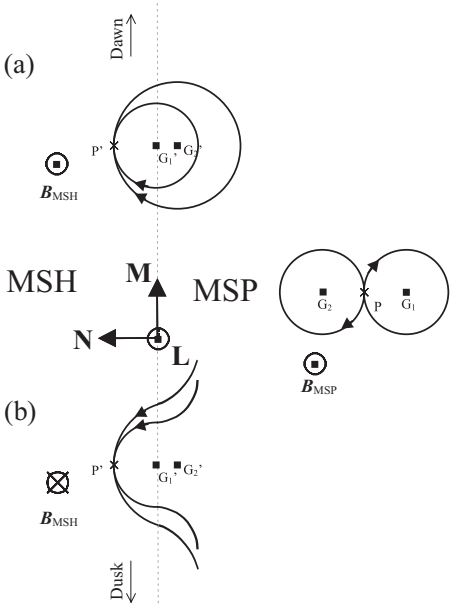

Fig. 5. Sketch of ion orbits for (**a**) northward and (**b**) southward IMF in the ($\boldsymbol{N}$, $\boldsymbol{M}$) plane when neglecting the effect of the convection, magnetic field-gradient and curvature drifts.

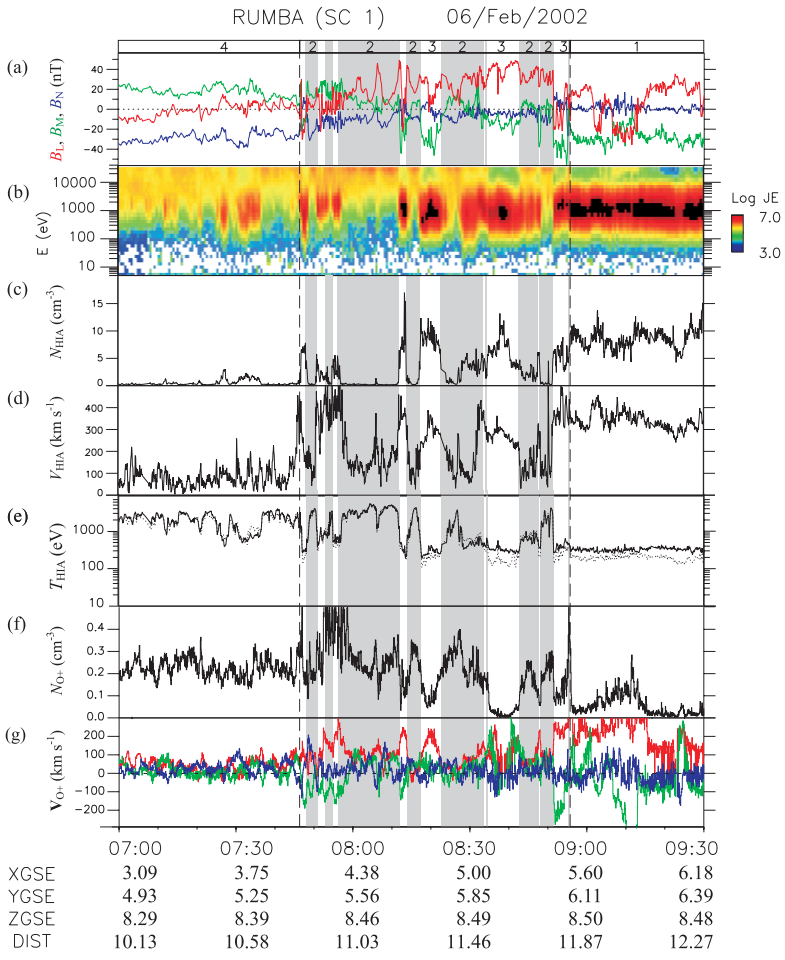

Fig. 6. Measurements in the MSP/MP/MSH from Cluster SC1 on 6 February 2002. The format is the same as in Fig. 3.

orientation of the MSH magnetic field, such energetic particles gyrate, entering ($V_N > 0$) or exiting ($V_N < 0$) the MSH, but have always $V_M < 0$. Conversely, for a northward orientation of the MSH magnetic field (Fig. 5a), energetic particles will gyrate, always having $V_M > 0$ on the MSH side. On the other hand, for a location P at distances larger than 2 O^+ gyroradii within the magnetosphere, ions may come from all directions and the isotropy of the distribution should be maintained. As usually observed in the near-MP regions (Eastman and Christon, 1995), O^+ energy distributions exhibit a power law shape at high energy with a spectral index ranging from -4 to -2. This indicates that for most of the time, the contribution at energies above 40 keV to the number density should be negligible, provided only measurements in the magnetosheath at distances of less than 2400 km from the MP are considered, which is always the case according to our selection criteria (see Sect. 2.2).

3.2 6 February 2002 case

Figure 6 shows one Cluster-SC1 outbound pass through the mid-latitude dusk flank of the MP that occurred on 6 February 2002. During the crossing, ACE data indicate a dynamic pressure that slightly fluctuates around a mean of 3.3 nPa. The IMF B_x component is negative and much stronger than the B_y component which is positive. The IMF B_z is steadily northward until 7:40 UT and then oscillates several times between -5 and 5 nT. SC1 is originally in the dayside plasma sheet, as evidenced by the presence of a hot, isotropic, ion component. From about 07:05 up to 07:35 UT, SC1 crossed several times bulges of MSH plasma of about a few minutes duration, as evidenced by the observation of intermediate densities and temperatures without any appreciable change in the B-field orientation. From 07:35 UT, SC1 crosses the MSHBL several times. Note that in this case, the plasma density in the MSH proper is relatively low ($5-10\,cm^{-3}$) while its velocity is higher than usual because of a fast solar wind flow (speed of $620\,km\,s^{-1}$) during the same period of time. The event is also characterized by very strong O^+ densities of about $0.2-0.5\,cm^{-3}$, which represents more than 90% of the mass density in the PS and MSPBL.

Figure 7 provides a detailed examination of 4-sresolution velocity distribution functions at two different times, when SC1 is located in the MSHBL (left-hand panels) and MSPBL (right-hand panels) under northward IMF conditions. Before

8:43:31 UT, SC1 is in the MSHBL (region 2) and truncated O^+ distributions are observed, i.e. only in the half-plane $V_M > 0$. As previously discussed in Sect. 3.2 from Fig. 5, this effect is due to the northward orientation of the MSH magnetic field. Note that velocity distributions in the (N, L) plane indicate that they are very scattered in pitch-angle, showing a component reflected at higher altitude or possibly flowing from the high-latitude ionosphere.

3.3 30 December 2001 case

Figure 8 shows one Cluster-SC1 outbound pass through the mid-latitude dusk flank of the MP that occurred on 30 December 2001. During the crossing, ACE data indicate steady northward IMF conditions and a very high dynamic pressure, which decrease from 7 to 4 nPa between 8:00 and 10:00 UT, and therefore would imply an outward MP motion. This possibly explains why the transition from the PS (region 4) to the MSH proper (region 1) is very slow in this case. The ion (without mass discrimination) and O^+ data are from HIA and CODIF with a resolution of 4 s for both. Another interesting feature in Fig. 8 is the presence of quasi-periodic fluctuations in the magnetic field components and plasma moments around 8:00 UT, between 8:55 and 9:15 UT, and between 9:38 and 9:50 UT. Such multiple and quasi-periodic encounters are often interpreted as the result of surface waves traveling along the MP region or vortices excited by the Kelvin-Helmholtz (KH) instability (Ogilvie and Fitzenreiter, 1989; Fairfield et al., 2000; Hasegawa et al., 2004), as we will see in Sect. 5. The event is also characterized by very strong O^+ densities, of about 0.2–0.5 cm^{-3}, which correspond to more than 90% of the mass density in the PS and MSPBL regions. Note that the velocity components are again very low in the PS and MSPBL regions, plots in the velocity space (not shown) indicating pitch-angle scattered distributions similar to those for the second event.

Table 1. List of mean parameters in the MSPBL and MSHBL inferred from the probability density functions of Fig. 10.

Parameter	MSPBL	MSHBL
H^+ number density (cm^{-3})	1.5	19.3
O^+ number density (cm^{-3})	0.041	0.007
O^+ mean energy (keV)	3.8	14.2
O^+ poleward velocity (km s^{-1})	58.4	117.4
O^+ normal velocity (km s^{-1})	0.5	3.2
Probability $P(r>1)$	0.140	≈0

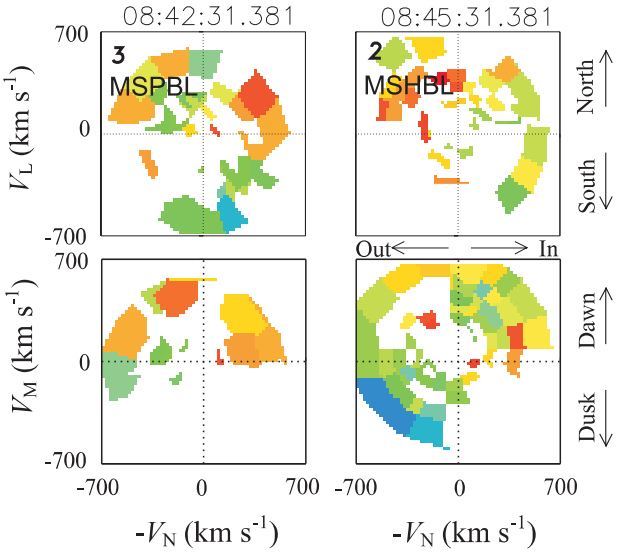

Fig. 7. From top to bottom, cutaway of the O^+ distribution function in the (N,L) plane at $V_M = <V_M>$ in Log[eV/(s cm^{2}sr eV)], in the (N,M) plane at $V_L = <V_L>$ in Log[eV/(s cm^{2}sr eV)]. The number in the topleft-hand side corner of each velocity distribution plot in the (N,L) plane refers to the region, according to Fig. 3.

4 Oxygen ion survey

We have selected all Cluster orbits from December 2000 to May 2003 that cross the dayside MP region, corresponding to a total number of 364 and 340 passes for SC1 and SC3, respectively. For each of these passes, we have repeated the procedure described in the flowchart of Fig. 2 to sort MSPBL and MSHBL crossings. Figure 9 shows the distribution in GSE local time φ and latitude λ of Cluster SC1 and SC3 data in the MSPBL and MSHBL. The total number of data points is 1.98×10^5 and 1.44×10^5 in the MSHBL and MSPBL regions, respectively. These measurements are binned in Fig. 9 using a resolution of $0.5h\times1°$. Note that data points are not uniformly distributed, with more measurements in the dusk-side than in the dawnside. To remove this spatial effect on the statistical results, any measurement within a bin (φ_i,λ_j) has been weighted by a normalization factor $1/N_{ij}$ where N_{ij} denotes the number of points inside the bin. On the other hand, mid-latitudes from 20° up to 60° are covered on both hemispheres, but the subsolar region is not scanned. Because all local times are scanned, it was possible to investigate potential dawn/dusk asymmetries in the results.

4.1 Probability distributions

Figure 10 shows the probability density functions of various parameters in the MSH and MSP transition layers integrated over all local times and latitudes. Such regions have been selected according to the flowchart of Fig. 2. First order moments from the probability density functions are summarized in Table 1. Because not all O^+ ions leak out across the MP, depending on their velocities along the normal, or when reconnection is active, such ions may be accelerated as well as reflected; the O^+ density N_O is found to be lower, by a factor of 6, in the MSHBL than in the MSPBL. Hence, only accelerated or energetic ions may escape, and the O^+ mean energy w_O and velocity components

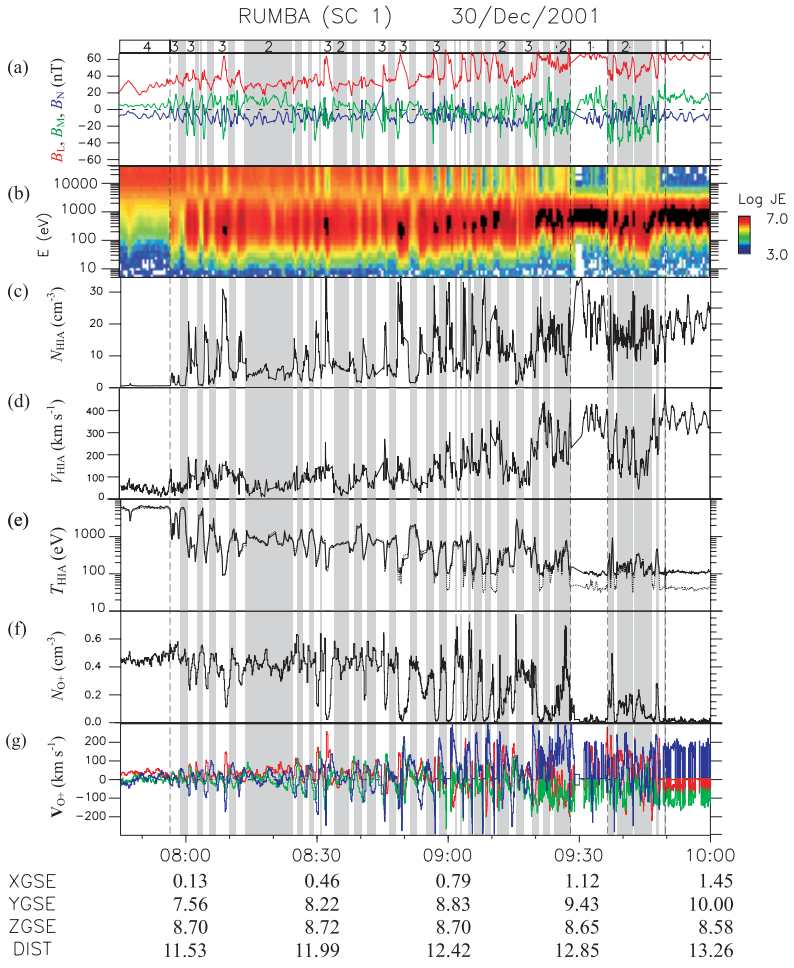

Fig. 8. Measurements in the MSP/MP/MSH from Cluster SC1 on 30 December 2001. The format is the same as in Fig. 3.

V_{ON} and V_{OP} are consequently higher in the MSHBL than in the MSPBL. Note that the profiles of the probability density function of V_{ON} exhibit a very large width, with standard deviations of 128 km s^{-1} and 72 km s^{-1} in the MSHBL and MSPBL regions, respectively. These values are rather large compared to the means so that there should be a substantial error in the average of V_{ON}. There are two factors that contribute to produce these broad distributions. First, potential errors in the normal determination scatter points around the mean velocity since the highest velocity component V_{OP} would not be projected correctly. Assuming an error of $\pm 10°$ in the normal leads to an apparent normal velocity $V_N^* = <V_{OP}> \times \sin(\pm 10°)$ equal to ± 10 km s^{-1} and to ± 20 km s^{-1} in the MSPBL and MSHBL, respectively. These numbers are, however, small compared to standard deviations. The second factor is due to the fact that we calculated the inertial velocity component adding the satellite velocity, which means that we did not deconvolve the effect of the MP motion in the probability distribution functions of O^+ velocities. Since earlier statistical studies showed that the MP moves at speeds ranging from 20 to 80 km s^{-1} (Haaland et al., 2004), this effect spreads significantly the probability density functions. Because the H^+ density N_H is much higher in the MSH than in the adjacent MSP region, the O^+/H^+ mass density ratio $r = \rho_O/\rho_H$ is found on average to be much larger in the MSPBL than in the MSHBL. When integrating such functions over the range $r > 1$, it is found that O^+ ions have a probability of 14.0% and nearly 0% chance of being the major constituent in the mass density in the MSPBL and MSHBL, respectively. The O^+ poleward velocity V_{OP} is equal in magnitude to the V_L component of the bulk velocity, but defined positive toward the poles, i.e. $V_{OP} = -V_L$ in the north while $V_{OP} = V_L$ in the south. Given the fact that the probability density function of V_{OP} mainly extends in the domain $V_{OP} > 0$ is consistent with the view that such ions are mainly of plasma sheet origin. However, the extension of the function in the domain $V_{OP} < 0$ points out the possible presence of a component directly injected from the high-latitude ionosphere or a reflected component.

4.2 Local time dependence

To investigate the dependence on local time, we split the results in three sectors: dawn (6–10 MLT), noon (10–14 MLT) and dusk (14–18). Table 2 summarizes the average O^+

Table 2. List of mean parameters in the dawn, noon and dusk magnetospheric transition layers inferred from the probability density functions of Fig. 10.

	MSPBL			MSHBL		
Parameter	Dawn	Noon	Dusk	Dawn	Noon	Dusk
O^+ number density (cm^{-3})	0.014	0.021	0.053	4×10^{-3}	6×10^{-3}	0.011
O^+ mean energy (keV)	4.28	3.62	3.85	14.6	14.0	14.4
O^+ poleward velocity (km s^{-1})	57.0	66.9	52.0	88.0	162.5	119.4
O^+ normal velocity (km s^{-1})	2.4	−17.2	5.1	34.8	−16.5	15.6
Probability $P(r>1)$	0.031	0.042	0.306	∼0	∼0	∼0

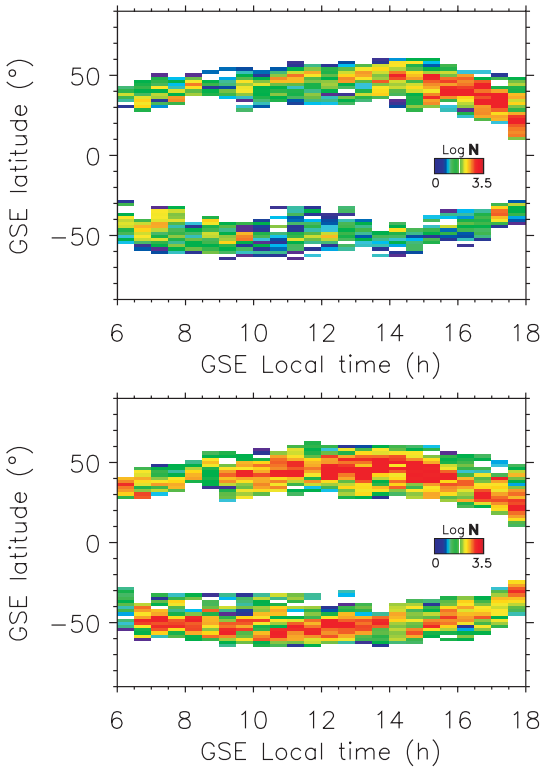

Fig. 9. Map of data points in the MSPBL (top) and MSHBL (bottom) from all crossings between December 2000 and May 2003 with SC1 and SC3 as a function of GSE local time and latitude. The color code is in Log of the number of samples per bin.

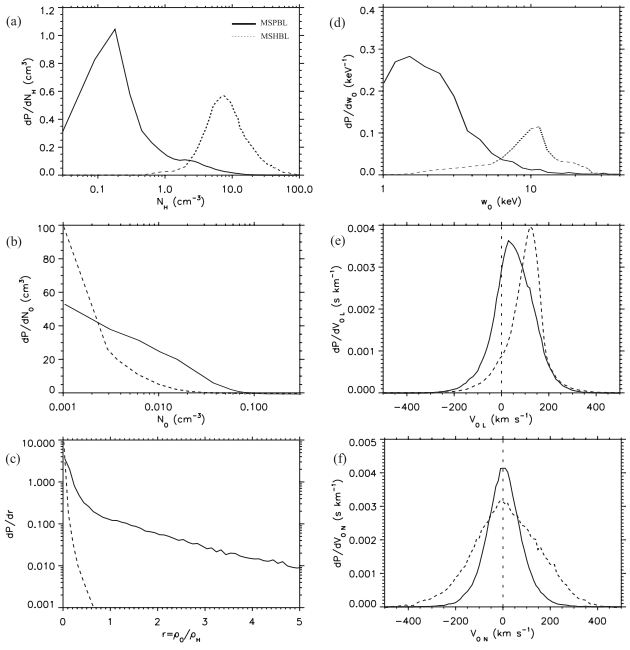

Fig. 10. Probability density functions in the magnetosheath (dot) and magnetosphere (solid) transition layers of (**a**) H^+ number density, (**b**) O^+ number density, (**c**) O^+/H^+ mass density ratio, (**d**) mean O^+ energy, (**e**) O^+ poleward velocity component, and (**f**) O^+ velocity component normal to the magnetopause.

moments in the MSPBL and MSHBL, inferred from the probability density functions in the different sectors. Note that the O^+ density is much larger in the dusk sector than anywhere else, as well as the O^+ contribution to the mass density. This result is consistent with the topology of the drift paths of energetic plasma sheet ions; from the midnight plasma sheet, such ions drift preferentially westward to hit the postnoon MP (Sibeck et al., 1987). The normal velocity is on average outward on the flanks, but found inward near noon, while other O^+ velocity components and the mean energy do not exhibit significant asymmetries. This artifact is related to the MP surface model. Indeed, the surface model is not appropriate when approaching the cusp funnel shape near noon, and the $\boldsymbol{L}$ velocity component is not calculated correctly and contributes to an apparent inward velocity component, i.e. in the $-\boldsymbol{N}$ direction.

4.3 Correlations with K_p and D_{st}*

It has long been known that O^+ outflowing fluxes at mid-altitudes increase with the geomagnetic activity, as monitored by the 3-hourly K_p index (Yau et al., 1988). So it is natural to ask if fluxes reaching the dayside MP region also depend on K_p. Figure 11 (right) shows the number densities of O^+ ions in the MSPBL and MSHBL as a function of K_p. A relation similar to the one inferred from mid-altitude obser-

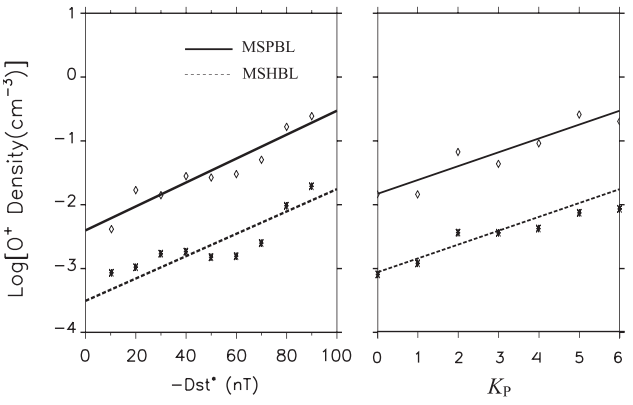

Fig. 11. Plot of the log of the average O^+ number density as a function of $-D_{st}{}^*$ (left) and K_p (right) in the MSPBL (solid line with diamonds) and MSHBL (dotted line with asterisks).

vations near solar maximum conditions (e.g. Yau et al., 1988) is found, with O^+ densities in the MSPBL and MSHBL increasing by a factor of 20 from K_p=0 to 6.

Since most of the O^+ ions in the near-MP region are of plasma sheet origin, we may expect that their densities vary with the strength of the ring current, as parametrized by the hourly disturbed storm time index D_{st}. However, we have utilized the modified disturbed storm time index $D_{st}{}^*$(see, for example, Tsyganenko, 2002), which differs from the standard D_{st} index by including the effect of the Earth's induction electric field and the magnetic field of the MP currents and is given by:

$$D^*_{st} = 0.8D_{st} - 13\sqrt{P_{\rm SW}}, \quad (1)$$

where P_{SW} denotes the solar wind dynamic pressure in nPa, while D_{st} and $D_{st}{}^*$ are in nT. Figure 11 (left) shows the number densities of O^+ ions in the MSPBL and MSHBL as a function of $D_{st}{}^*$. Note that we did not extend the study to strong storms where $D_{st}{}^*$ is lower than -100 nT, because the number of such events is too small to provide good statistics. The O^+ densities increase exponentially with $-D_{st}{}^*$, by about two orders of magnitude from $D_{st}{}^*$=$-$100 to 0 nT.

4.4 Loss rate

Since we have shown that a non-negligible fraction ($\sim$1/6) of O^+ ions is lost across the MP in the magnetosheath, it is interesting to provide loss rate estimations and compare the values with loss rates from other magnetospheric regions. Since the leakage is expected to be more significant at equatorial latitudes, which are not covered in our study, our calculation would give a lower limit of the loss rates.

There are two ways to estimate the loss rate. One is by integrating the normal flux across the dayside MP, assimilating the surface as half a sphere of radius r_0=10.3 R_E and assuming that leakage occurs over all latitudes below 60°. Then the average loss rate is given by $I=\pi\times3^{1/2}\times r_0^2\times<N_O><V_{0N}>$, where $<N_0>$ and $<V_{0N}>$ are the average O^+ density and normal velocity, respectively. This method is not accurate because of the large error in the average normal velocity $<V_{0N}>$, using the results of Sect. 4.1. Alternatively, as calculated in Seki et al. (2001), one can have an estimation of the loss rate, assuming that all ions in the magnetosheath were leaking with a jet velocity $<V_{0P}>$=117.4 km s^{-1} (see Table 1) in a transition layer extending over the whole dayside MP (longitudinal range: 180°, length: $\pi\times r_0$) with a radial thickness l of about 2 O^+ gyroradii ($l\sim1\,R_E$). Then, the resultant O^+ loss is $I=\pi\times r_0\times l\times<N_O><V_{0P}>\sim1.1\times10^{24}$ ions s^{-1}. To find the same number using the first method, we would need an average normal velocity $<V_{0N}>\sim$6.5 km s^{-1}, which is a reasonable value.

The inferred loss rate across the dayside MP is of the same order as the O^+ loss rate in the nightside magnetosphere (Seki et al., 2001), and one order of magnitude lower than the one inferred from mid-altitude and high-latitude data at solar maximum (Yau et al., 1988).

5 Discussion: Influence of O^+ ions on physical magnetopause processes

In addition to their role in determining plasma sources, O^+ ions, when a substantial amount is present, may play an active role in the physical processes acting in the near-MP regions. Indeed, because we pointed out in Sect. 4 that O^+ ions have a non-negligible probability to dominate the mass composition in the duskside MP, a preferred region for the Kelvin-Helmholtz (KH) instability, we investigate its role when such an instability is able to grow. We also discuss here the influence of a significant O^+ ion component on other processes such as magnetic reconnection.

5.1 Kelvin-Helmholtz instability generation

The Kelvin-Helmholtz instability appears in a fluid flow in the presence of a shear velocity. Due to the shear imposed by the magnetosheath plasma flowing around the magnetosphere, the MP flanks are preferred regions for the generation of the KH instability. In the classical magnetohydrodynamic (MHD) framework, considering that the plasma is homogeneous on both sides of the MP and using a planar wave with wave vector $\boldsymbol{k}$, the criterion for KH instability can be expressed as (Hasegawa, 1975):

$$(\mathbf{k}\cdot\Delta\mathbf{V})^2 > \left(\frac{1}{\rho_2}+\frac{1}{\rho_3}\right)\left[(\mathbf{k}\cdot\mathbf{V}_{A\,2})^2+(\mathbf{k}\cdot\mathbf{V}_{A\,3})^2\right], \quad (2)$$

where the subscripts 2 and 3 refer to the MSHBL and MSPBL, and $\Delta\boldsymbol{V}=\boldsymbol{V}_2-\boldsymbol{V}_3$ is the shear velocity. $\boldsymbol{V}_{A2}$ and $\boldsymbol{V}_{A3}$ denote the Alfvén speed in the MSHBL and MSPBL, respectively. Note that ρ_2, ρ_3, $\boldsymbol{V}_2$ and $\boldsymbol{V}_3$ correspond to one-fluid plasma moments. From Eq. (2), as Hasegawa (1975) points out, the most unstable situation would be when $\boldsymbol{k}$ is parallel to $\Delta\boldsymbol{V}$ and perpendicular to $\boldsymbol{B}$. These criteria allow us to make definite predictions concerning the location and

condition under which the instability is expected, as we will see now for a case study in the dusk-side MP.

Figure 12 provides a closer look at single-fluid moments from SC1 when surface waves are observed on 30 December 2001 (see Sect. 3.3). Plasma transfer across the MP is also observed in Fig. 12b since indeed, cold magnetosheath ions (<3 keV) and hot magnetospheric O^+ ions (>5 keV) coexist whenever the spacecraft returns to the MSPBL (gray intervals). As evidenced in Fig. 12c, the major effect of considering the O^+ component is to increase the mass density in the MSPBL and therefore to lower the drop in mass density across the MP. Figure 12d indicates that the shear flow is mainly along $-\boldsymbol{M}$. The criterion for instability may also be tested in the case where $\boldsymbol{k}$ //$-\boldsymbol{M}$, and is then expressed as:

$$|\Delta V_M| > \left(\frac{B_{M2}^2 + B_{M3}^2}{\mu_0 \rho^*} \right)^{1/2}, \quad (3)$$

where ρ^*=$\rho_2\rho_3/(\rho_2+\rho_3)$ and B_{M2}, B_{M3} denote the magnetic field components along $\boldsymbol{M}$ in the MSHBL and MSPBL, respectively.

We have tested Eq. (3) for each MP crossing marked by an arrow in Fig. 12a, from 8:56:53 to 9:09:50 UT, in order to determine if the KH instability was operating at these boundaries. Here, ΔV_M was defined as the difference between the velocity maximum and minimum across each individual MP crossing, while other parameters were set taking the extrema in the MSPBL and MSHBL sides. Figure 13 shows scatterplots of the velocity shear ΔV_M as a function of the velocity threshold given by the right-hand side of Eq. (3) when including and without considering the O^+ component in the calculation of ρ^*. We clearly see that adding the O^+ component in the calculation helps to lower the velocity threshold so that the MP boundary is KH-unstable.

6 Influence on magnetic reconnection

There are other physical processes that strongly depend on the mass density, such as, for example, magnetic reconnection. When a substantial amount of O^+ ions is present, the mass density increases appreciably. In addition, such heavy ions will add a hierarchy of new scales to the dissipation region near the reconnection X-line by increasing the ion mean gyroradius and ion inertial length, and will tend to slow down the Alfvén speed V_A. As reported by Shay and Swidsak (2004) in studying the effect of O^+ in the magnetotail reconnection region, there are two larger length scales in the system: one associated with a "heavy whistler" which produces a large-scale, quadrupolar, out-of-plane magnetic field, and one associated with a "heavy Alfvén" wave which can decrease the inflow speed and thus the reconnection rate. Furthermore, numerical simulation studies show that fast reconnection can be triggered when the thickness of the current sheet is reduced to the order of the ion inertial length (Scholer et al., 2003). Under the presence of O^+ ions, reconnection may be induced even for a thick current sheet, although the reconnection rate itself may be reduced.

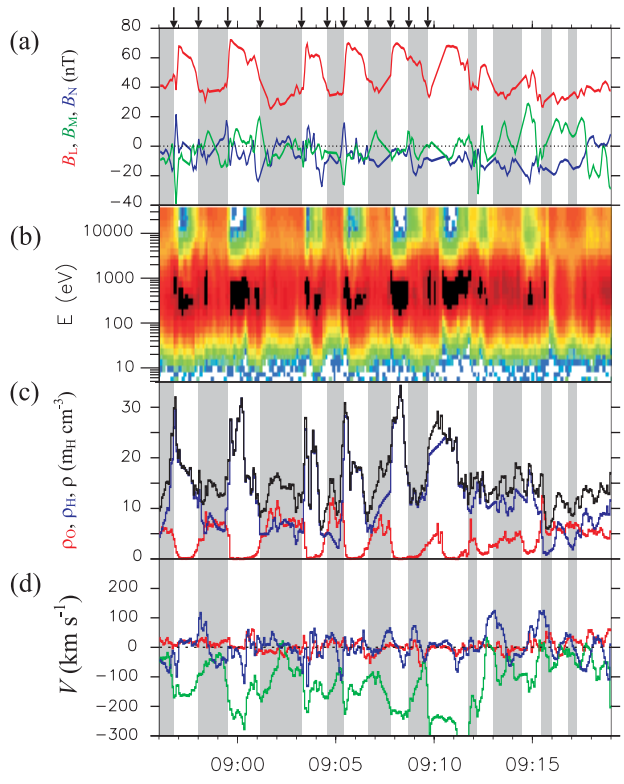

Fig. 12. Closer look at the measurements on 30 December 2001 from 8:56:00 to 9:19:00 UT. (**a**) Magnetic field components in the LMN frame; (**b**) ion energy-time spectrogram in Log[eV/(s cm^{2}sr eV)] from HIA; (**c**) O^+ (red), H^+ (blue), and total (black) mass density of in cm^{-3} from HIA; and (**d**) single-fluid velocities in the LMN frame in km s^{-1}. L, M, and N components are plotted in red, green and blue, respectively.

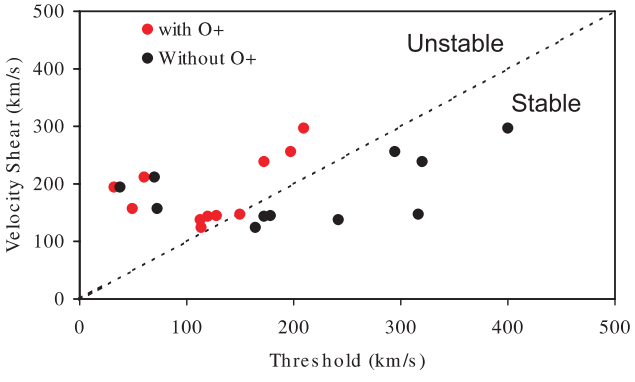

Fig. 13. Scatterplots of the shear flow velocity as a function of the velocity threshold given by the right-hand side of Eq. (3) when considering H^+ ions only (black rounds) and when adding the O^+ component (red rounds) into the calculation. In the region above the dotted line, the instability criterion is satisfied.

Another possible suggestion with regard to this topic has been made by Baker et al. (1982, 1985), showing that O^+ ions could help to determine the pattern of initiation of plasma sheet instabilities during substorms. This sugges-

tion was based on the theoretical expectation that a region of the plasma sheet dominated by O^+ rather than H^+ ions would have a lower threshold and a larger growth rate for the ion tearing mode instability, in a similar way to that made here for the KH instability. In turn, the tearing mode would give rise to the macroscopic neutral line associated with substorm expansion onset. Then, a relatively localized region of oxygen-dominated plasma might be the most likely region where the substorm would develop. The fact that O^+ densities are found to be higher in the dusk-side and strongly K_p-dependent in our paper is at least compatible with this possible scenario.

7 Summary and conclusions

In this paper, we presented a comprehensive survey of O^+ ion measurements at energies ranging from 30 eV up to 40 keV in the dayside, mid-latitude, near-magnetopause (MP) region. The main results are as follows:

1. The O^+ density decreases by a factor of 6 across the MP, from 0.041 cm^{-3} in the magnetospheric boundary layer (MSPBL) down to 7.0×10^{-3} cm^{-3} in the magnetosheath boundary layer (MSHBL).

2. The lower limit of the loss rate of O^+ ions across the dayside MP is about 2.4×10^{24} ions s^{-1} at solar maximum. This number is comparable to the loss rate of O^+ ions in the nightside magnetosphere (Seki et al., 2001), but one order of magnitude lower than the loss rate across the mid-altitude polar caps (Yau et al., 1988), supporting the view that there is a substantial return flux from the magnetosphere to the low-latitude ionosphere, as suggested by Seki et al. (2001).

3. Strong dawn-dusk asymmetries are found in terms of density, which are related to the topology of the drift paths between the nightside plasma sheet and the dayside MP. In particular, inward of the magnetopause, O^+ is the dominant contributor to the mass density 30% of the time in the dusk-side compared to 3% in the dawn-side MSPBL.

4. The O^+ content near the MP depends strongly on the geomagnetic activity and strength of the ring current in the same way as in the mid-altitude polar cap, with densities varying exponentially with the K_p and modified $D_{st}{}^*$ indexes.

Beyond accessing plasma sources and losses in the near MP regions, the fact that O^+ ions may dominate the mass density of the plasma has some implications in terms of physical MP processes. On an event basis, where high O^+ densities were observed in the presence of wave fluctuations, consistent with the presence of KH waves (a detailed analysis of this event is to be reported in future), we pointed out that O^+ ions, when substantially present in the mass composition in the dusk-side MP, decrease the velocity threshold so that a lower magnetosheath shear flow enables the excitation of the Kelvin-Helmholtz (KH) instability. On the other hand, we have also shown qualitatively that significant densities of O^+ ions in a reconnection region would slow down the Alfvén speed and reduce the reconnection rate after introducing a hierarchy of new scales in the diffusion region, as suggested by Shay and Swidsak (2004) when studying the effect of heavy ions in magnetotail reconnection.

The fact that O^+ ions are able to influence physical MP processes suggests that they should be taken into consideration in global magnetospheric models. Global multi-fluid simulations including the O^+ ion component, have already been developed (Winglee et al., 2002). However, they do not spatially resolve the reconnection boundaries yet. Other MHD simulations have examined the acceleration of O^+ test particles in the presence of an KH instability developing at the MP (Smets et al., 2002), but without taking them into account self-consistently. Because all these MP physical processes have a significant impact on macroscopic scales, incorporating the effect of the O^+ component on such MP processes would be an important challenge.

Appendix A

Because the HIA instrument sorts ions according to energy per charge, it does not resolve different ion species. For the on-board moment computation, where energies have to be converted into velocities, it is assumed that all ions are protons. If heavy ions of mass m_i and charge Q_i are present, their velocity would be overestimated by a factor $\gamma=[m_i/(Q_i m_H)]^{1/2}$, while their density will be underestimated by the same factor.

Let us assume that the ion population consists of three main species, H^+, He^{++} and O^+, with densities N_H, N_{He} and N_O, and bulk velocities $\boldsymbol{V}_H$, $\boldsymbol{V}_{He}$, and $\boldsymbol{V}_O$. The HIA instrument measures the apparent moments (Paschmann et al., 1986):

$$N^* = N_H + N_{He}\Big/\sqrt{2} + N_O\big/4 \tag{A1}$$

$$\mathbf{V}^* = \frac{1}{N^*}\left(N_H\mathbf{V}_H + N_{He}\mathbf{V}_{He} + N_O\mathbf{V}_O\right). \tag{A2}$$

Because He^{++} moments are generally difficult to measure with CODIF (Rème et al., 2001), we need to assume a fixed $K_{He}=N_{He}/N_H$ density ratio and $\boldsymbol{V}_{He}=\boldsymbol{V}_H$, which is a reasonable assumption (Paschmann et al., 1989). Hence, knowing $(N_O,\boldsymbol{V}_O)$ from CODIF and $(N^*,\boldsymbol{V}^*)$ from HIA and setting K_{He}=0.04, which corresponds to the average ratio in the solar wind, the H^+ moments may be inferred using Eqs. (A1) and (A2):

$$N_H = \frac{N^* - N_O\big/4}{1 + K_{He}\Big/\sqrt{2}} \tag{A3}$$

$$\mathbf{V}_H = \frac{1}{N_H\,(1+K_{He})}\left(N^*\mathbf{V}^* - N_O\mathbf{V}_O\right). \tag{A4}$$

Note in Eqs. (A3) and (A4) that the introduction of an He^{++} component acts as a second order correction, lowering the H^+ density and bulk velocity by about 3 and 4%, respectively.

Knowing H^+ moments from Eqs. (A3) and (A4), single-fluid moments, i.e. density N, mass density ρ, and velocity $\boldsymbol{V}$, may be inferred in the following way:

$$N = \sum_i N_i = (1 + K_{He})\, N_H + N_O \tag{A5}$$

$$\rho = \sum_i \rho_i = m_H\, [(1 + 2K_{He})\, N_H + 16 N_O] \tag{A6}$$

$$\mathbf{V} = \frac{1}{\rho} \sum_i \rho_i \mathbf{V}_i = \frac{(1 + 2K_{He})\, N_H \mathbf{V}_H + 16 N_O \mathbf{V}_O}{(1 + 2K_{He})\, N_H + 16 N_O}. \tag{A7}$$

Acknowledgements. We are grateful to the technical and scientific personnel at MPE, Garching; CESR, Toulouse, UNH, Durham; IFSI, Frascati; IRF, Kiruna; MPS, Lindau; UCB, Berkeley; and UW, Seattle; who made the development of the CIS instrument possible. The work at MPE in Garching is supported by DLR (Deutsches Zentrum für Luft und Raumfahrt) under contract 50 OC 0102. We thank all people who contributed to the OMNIWeb database of the National Space Science Data Center (NSSDC).

Topical Editor T. Pulkkinen thanks K. Seki and another referee for their help in evaluating this paper.

References

Baker, D. N., Hones, E. W. Jr., Young, D. T., and Birn, J.: The possible role of ionospheric oxygen in the initiation and development of plasma sheet instabilities, Geophys. Res. Lett., 9, 1337–1340, 1982.

Baker, D. N., Fritz, T. A., Lennartsson, W., Wilken, B., Kroehl, H. W., and Birn, J.: The role of heavy ionospheric ions in the localization of substorm disturbances on 22 March 1979: CDAW 6, J. Geophys. Res., 90, 1273–1281, 1985.

Balogh, A., Carr, C. M., and Acuña, M. H., et al.: The Cluster Magnetic Field Investigation: Overview of in-flight performance and initial results, Ann. Geophys., 19, 1207–1217, 2001, **SRef-ID: 1432-0576/ag/2001-19-1207**.

Eastman, T. and Christon, S.: Ion composition and transport near the Earth's magnetopause, in Physics of the magnetopause, Geophys. Monogr. Ser., vol. 90, edited by: Song, P., Sonnerup, B. U. Ö., and Thomsen, M. F., 131–137, AGU, Washington DC, 1995.

Fairfield, D. H., Otto, A., Mukai, T., Kokobun, S., Lepping, R. P., Steinberg, J. T., Lazarus, A. J., and Yamamoto, T.: Geotail observations of the Kelvin-Helmholtz instability at the equatorial magnetotail boundary for parallel northward fields, J. Geophys. Res., 105, 21 159–21 174, 2000.

Fuselier, S. A., Klumpar, D. M., Peterson, W. K., and Shelley, E. G. : Direct injection of ionospheric O^+ ions into the dayside low-latitude boundary layer, Geophys. Res. Lett., 16, 1121–1124, 1989.

Fuselier, S. A., Klumpar, D. M., and Shelley, E. G.: On the origins of energetic ions in the Earth's dayside magnetosheath, J. Geophys. Res., 96, 47–56, 1991.

Haaland, S. E., Sonnerup, B. U. Ö., and Dunlop, M. W., et al.: Four spacecraft determination of magnetopause orientation, motion and thickness: Comparison with results from single-spacecraft methods, Ann. Geophys., 22, 1347–1365, 2004, **SRef-ID: 1432-0576/ag/2004-22-1347**.

Hasegawa, A.: Plasma instabilities and non-linear effects, Springer-Verlag, New York, 1975.

Hasegawa, H., Fujimoto, M., Phan, T. D., Rème, H., Balogh, A., Dunlop, M. W., Hashimoto, C., and TanDokoro, R.: Transport of solar wind ions into Earth's magnetosphere through rolled-up Kelvin-Helmholtz vortices, Nature, 430, 755–758, 2004.

Hultqvist, B., Øieroset, M., Paschmann, G., and Treumann, R.: Magnetospheric plasma sources and losses, Space Sci. Rev., 88, 7–84, 1999.

Kudela, K., Sibeck, D. G., and Slivka, M.: Prognoz 10 energetic particle data: Leakage from the magnetosphere versus bow shock acceleration, J. Geophys. Res., 99, 23 461–23 472, 1994.

Lundin, R. and Dubinin, E. M.: Solar wind energy transfer regions inside the dayside magnetopause: Accelerated heavy ions as tracers for MHD-processes in the dayside boundary layer, Planet. Space Sci., 33, 891–907, 1985.

Marcucci, M. F., Bavassano-Cattaneo, M. B., and Pallochia, G. et al.: Magnetospheric oxygen in the magnetosheath and its response to IMF orientation: Cluster observations, J. Geophys. Res., 109(A07203), doi:10.1029/2003JA010312, 2004.

Ogilvie, K. W. and Fitzenreiter, R. J.: The Kelvin-Helmholtz instability at the magnetopause and inner boundary layer surface, J. Geophys. Res., 94, 15 113–15 123, 1989.

Paschmann, G., Pamastorakis, I., Baumjohann et al.: The magnetopause for large magnetic shear: AMPTE/IRM observations, J. Geophys. Res., 91, 11 099–11 115, 1986.

Paschmann, G., Fuselier, S. A., and Klumpar, D. M.: High-speed flows of H^+ and He^{++} ions at the magnetopause, Geophys. Res. Lett., 16, 567–570, 1989.

Paschmann, G.: Observational evidence for transfer of plasma across the magnetopause, Space Sci. Rev., 80, 217–234, 1997.

Paschmann, G. and Daly, P.: Analysis methods for multispacecraft data, ISSI scientific reports, Bern, 2000.

Peterson, W. K., Shelley, E. G., Haerendel, G., and Paschmann, G.: Energetic ion composition in the subsolar magnetopause and boundary layer, J. Geophys. Res., 87, 2139–2145, 1982.

Phan, T. D., Paschmann, G., Baumjohann, W., Sckopke, N., and Lühr, H.: The magnetosheath region adjacent to the dayside magnetopause: AMPTE/IRM observations, J. Geophys. Res., 99, 121–141, 1995.

Phan, T. D., Paschmann, G., and Sonnerup, B. U. Ö.: Low-latitude dayside magnetopause and boundary layer for high magnetic shear. 2 Occurrence of magnetic reconnection, J. Geophys. Res., 101, 7817–7828, 1996.

Phan, T. D., Dunlop, M. W., Paschmann, G. et al.: Cluster observations of continuous reconnection at the magnetopause under steady interplanetary magnetic field conditions, Ann. Geophys., 22, 2355–2367, 2004, **SRef-ID: 1432-0576/ag/2004-22-2355**.

Rème, H., Aoustin, C., and Bosqued, J.-M. et al.: First multispacecraft ion measurements in and near the Earth's magnetosphere with the identical Cluster ion spectrometry (CIS) experiment, Ann. Geophys., 19, 1303–1354, 2001, **SRef-ID: 1432-0576/ag/2001-19-1303**.

Russell, C. T. and Elphic, R. C.: ISEE observations of flux transfer events at the dayside magnetopause, Geophys. Res. Lett., 6, 33–36, 1979.

Sauvaud, J.-A., Lundin, R., and Rème, H. et al.: Intermittent thermal plasma acceleration linked to sporadic motions of the magnetopause, first Cluster results, Ann. Geophys., 19, 1523–1532,

2001, **SRef-ID: 1432-0576/ag/2001-19-1523**.

Scholer, M.: Energetic particle signatures near magnetospheric boundaries, J. of Geophys., 52, 176–189, 1983.

Scholer, M., Sidorenko, I., Jaroschek, C. H., Treumann, R. A., and Zeiler, A.: Onset of collisionless magnetic reconnection in thin current sheets: Three-dimensional particle simulations, Phys. Plasmas, 10, 3521–3527, 2003.

Seki, K., Hirahara, M., and Teresawa, T. et al.: Statistical properties and possible supply mechanisms of tailward cold O^+ beams in the lobe/mantle regions, J. Geophys. Res., 103, 4477–4489, 1998.

Seki, K., Elphic, R. C., Hirahara, M., Terasawa, T., and Mukai, T.: On atmospheric loss of oxygen ions from Earth through magnetospheric processes, Science, 291, 1939-1941, 2001.

Seki, K., Elphic, R. C., Thomsen, M. F., Bonnell, J., McFadden, J. P., Lund, E. J., Hirahara, M., Terasawa, T., and Mukai, T.: A new perspective on plasma supply mechanisms to the magnetotail from a statistical comparison of dayside mirroring O^+ at low altitudes with lobe/mantle beams, J. Geophys. Res., 107(A4), doi:10.1029/2001JA900122, 2002.

Shay, M. A. and Swisdak, M.: Three-species collisionless reconnection: Effect of O^+ on magnetotail reconnection, Phys. Rev. Lett., 93(17), 175 001, 2004.

Shelley, E. G., Johnson, R. G., and Sharp, R. D.: Satellite observations of energetic heavy ions during a geomagnetic storm, J. Geophys. Res., 77, 6104–6110, 1972.

Shue, J.-H., Chao, J. K., and Fu, H. C. et al.: A new functional form to study the solar wind control of the magnetopause size and shape, J. Geophys. Res., 102, 9497–9511, 1997.

Sibeck, D. G., McEntire, R. W., and Lui, A. et al.: Energetic magnetospheric ions at the dayside magnetopause: Leakage or merging? J. Geophys. Res., 92, 12 097–12 114, 1987.

Smets, R., Delcourt, D., Chanteur, G., and Moore, T. E.: On the incidence of Kelvin-Helmholtz instability for mass exchange process at the Earth's magnetopause, Ann. Geophys., 20, 757–769, 2002,
SRef-ID: 1432-0576/ag/2002-20-757.

Speiser, T. G., Williams, D. J., and Garcia, H. A.: Magnetospherically trapped ions as a source of magnetosheath energetic ions, J. Geophys. Res., 86, 723–732, 1981.

Tsyganenko, N. A.: A model of the near magnetosphere with a dawn-dusk asymmetry 2. Parameterization and fitting to observations, J. Geophys. Res., 107(A8), doi:10.1029/2001JA000220, 2002.

Winglee, R. M., Chua, D., Brittnacher, M., Parks, G. K., and Lu, G.: Global impact of ionospheric outflows on the dynamics of the magnetosphere and cross-polar cap potential, J. Geophys. Res., 107, 1237, doi:10.1029/2001JA000214, 2002.

Yau, A. W., Peterson, W. K., and Shelley, E. G.: Quantitative parametrization of energetic ionospheric outflow, in modeling magnetospheric plasma, Geophys. Monogr. Ser., vol. 44, edited by: Moore, T. E., and Waite, J. H., AGU, Washington D.C., 211–217, 1988.

Yau, A. W. and André, M.: Sources of ion outflow, Space Sci. Rev., 80, 1–25, 1997.

Zong, Q.-G. and Wilken, B.: Layered structure of energetic oxygen ions in the dayside magnetosheath, Geophys. Res. Lett., 25, 4121–4124, 1998.